

Comitato Nazionale per l'Energia Nucleare
ISTITUTO NAZIONALE DI FISICA NUCLEARE

Sezione di Padova
63/2

INFN/BE-63/4
18 Luglio 1963.

G. Pisent: CORRECTIONS OF NEUTRON SPECTRA IN A RECOIL
CHAMBER.

Reparto Tipografico
dei Laboratori Nazionali di Frascati
Cas. Postale 70 - Frascati (Roma)

INFN/BE-63/4
18 Luglio 1963.

G. Pisent. CORRECTIONS OF NEUTRON SPECTRA IN A RECOIL CHAMBER^(x).

1. It is well known that the differential cross section of neutrons scattered elastically by light nuclei in the centre of mass system can be deduced from measurements of the energy spectrum of the recoil nuclei. The spectrum is in general deformed by various effects connected with the geometrical and electrical characteristics of the system of detection. Corrections to be applied must be evaluated with much care, especially when the differential cross section has to be analysed into its spherical harmonic components. The main difficulty encountered, when one tries to extract the "true" cross section σ from the experimental cross section σ_{exp} , lies in the fact that the amount of corrections is a function of σ itself, which is unknown.

A method is given herein for the solution of this problem. The method has been applied with good results to an alpha particle recoil counter^(1, 2).

2. Be

$$(1) \quad \sigma(\theta) = \sum_{n=0}^{2L_{\text{max}}} A_n \cos^n \theta$$

(x) - This work has been carried out under contract Euratom-Cnen.

2.

the differential cross section (Θ = scattering angle in the CM system; L_{\max} = maximum angular momentum involved at the considered energy). By the transformation $x = E/E_0 = 1/2 (1 - \cos \Theta)$ (E = energy of the recoiling ion; E_0 = energy of the recoiling ion for a head on collision), the angular distribution can be correlated with the energy spectrum of the recoil nuclei. Namely

$$(2) \quad \sigma(x) = \sum_{n=0}^{2L_{\max}} B_n x^n,$$

where

$$(3) \quad B_n = (-2)^n \sum_{i=n}^{2L_{\max}} \frac{i!}{n!(i-n)!} A_i$$

Let us now suppose that the pulses relative to a channel $y, y + dy$ be spread along contiguous channels, according to a distribution law $P(y, z)$. In this case the actual distribution, detected by the system, becomes

$$(4) \quad \sigma_{\text{exp}}(x) = \int_0^1 K(y) P(y, x) dy,$$

where the normalization factor $K(y)$ is calculated from the obvious condition:

$$K(y) \int_0^1 P(y, x) dx = G(y)$$

From Eq. (2) one obtains

$$(5) \quad \sigma_{\text{exp}}(x) = \sum_{n=0}^{2L_{\max}} B_n f_n(x),$$

where the functions

$$(6) \quad f_n(x) = \frac{\int_0^1 y^n P(y, x) dy}{\int_0^1 P(y, x) dx}$$

are known if the effect responsible for the spread in energy is known. A least squares analysis of the experimental distribution, by means of expression (5), allows a straightforward calculation of the coefficients B_n , and consequently of $\mathcal{G}(x)$ through Eq. (2). It must be pointed out that the correction depends on L_{\max} , and is "exact" if no angular momentum higher than L_{\max} is present.

The general formula (5) can be applied to any kind of distribution function $P(y, z)$. In the following sections some cases of practical interest will be discussed in detail, and the explicit form of the $f_n(x)$ will be given for a coaxial cylindrical chamber.

3. Owing to the induction of positive ions, the height of the electronic pulse, produced by the ionization of the recoil nucleus, is in general a function of the space coordinates. In an ungridded cylindrical chamber the radial dependence of the pulse height is

$$(7) \quad x(r) = \rho(r) / \rho(b),$$

($\rho(u) = 2 \ln(u/a)$; a and b are the radii of the internal and external electrode respectively)⁽³⁾. By means of Eq. (7) the $f_n(x)$ can be easily calculated.

$$(8) \quad f_n(x) = \frac{x^n \rho(b)^{n+1}}{\exp[\rho(b)] - 1} \left\{ \lambda_n[\rho(b)] - \lambda_n[x\rho(b)] \right\}$$

for $0 \leq x \leq 1$

and $f_n(x) = 0$ for $x > 1$,

where

$$(9a) \quad \lambda_n(u) = n^{-1} \left[\lambda_{n-1}(u) - \exp u/u^n \right],$$

$$(9b) \quad \lambda_0(u) = \bar{E}_i(u),$$

4.

$(\bar{E}_i(u) = \int_{-\infty}^u [\exp u/u] du$ is the exponential integral tabulated by Jahnke and Emde).⁽⁺⁾

In Fig. 1 the shape of the $f_n(x)$ up to P waves is shown for $b/a = 100$ and $b/a = \infty$.

4. Since the dimension of the chamber are not infinite, to evaluate $\phi(\theta)$ one has to consider the effect of both the tracks leaving the counter and those entering the counter being generated out of it.

The geometry of a cylindrical chamber, with the neutron beam parallel to its longitudinal axis, has been studied by Rossi and Staub⁽⁴⁾ and by Skyrme et al. ⁽⁵⁾ in the case of an S wave interaction (proton recoil chamber). The S and P waves approximation (deuteron recoil chamber) has been considered by Tunnicliffe⁽⁶⁾ under simplified assumptions (a linear energy dependence of the range of the recoiling ions).

The generalization of Skyrme's formulas to any angular momentum is straightforward, following the procedure presented in Section 2. The $f_n(x)$ functions can be written in a very general form without specifying the form of the range-energy relation.

$$(10) \quad f_n(x) = x^n + (R_0/b)\alpha_n(x) + (R_0/c)\beta_n(x) + (R_0^2/[bc])\gamma_n(x)$$

$$\text{for } 0 \leq x \leq 1$$

$$\text{and } f_n(x) = 0 \quad \text{for } x > 1,$$

where

$$(11a) \quad \alpha_n(x) = [2/\pi] \left[\int_x^1 y^n \sqrt{1-y} R'(y-x) dy - x^n \sqrt{1-x} R(x) \right],$$

(+) If tabulated values are not sufficient for the evaluation of the rapidly varying function $\lambda_0(x)$, the following slowly converging series can be employed:

$$\int [\exp u/u] du = C + \ln u + \sum_{i=1}^{\infty} \frac{u^i}{i \cdot i!}$$

$$\beta_n(x) = \int_x^1 y^{n+1/2} R'(y-x) dy - x^{n+1/2} R(x) +$$

$$(11b) \quad + \frac{2}{2n+3} R'(x) (1-x^{n+3/2}),$$

$$\gamma_n(x) = [2/\pi] [x^{n+1/2} \sqrt{1-x} R^2(x) +$$

$$(11c) \quad + \int_x^1 y^{n+1/2} \sqrt{1-y} \{ 2R(y-x) R'(y-x) - 2R(y) R'(y-x) -$$

$$- R'(x) R(y) + \int_x^y R'(y+x-z) R'(y-z) dz \} dy],$$

(R_0 = maximum range of the recoiling ions; $R(u)$ = range of the ion whose energy is $E = uE_0$, expressed in units R_0 ; $R'(u) = dR(u)/du$; c = length of the cylinder). A knowledge of the range-energy relation is required for the calculation of the integrals contained in Eq. (11). It is well known that, for slow heavy particles, the theory of the stopping power leads to unsatisfactory results, particularly because of the capture and loss of electrons by particles. The functions $\alpha_n(x)$, $\beta_n(x)$, $\gamma_n(x)$, have been computed using the empirical range-energy relationship given by Bethe⁽⁷⁾ for alpha particles in air. These results, relative to S, P and D waves, and alpha energies $E_0 = 1, 2, 4$ and 8 MeV are reported in tables I through IV. These tables can be interpolated for other energies. For protons, deuterons and tritons, the given values can be used by a proper choice of E_0 , taking into account the approximate relation

$$R_M(E_0) = M/(M_p Z^2) R_p(E_0 M_p/M)$$

(R_M = maximum range of the particle of mass M and charge $Z e$; R_p and M_p are the maximum range and the mass of the proton; see for example⁽⁸⁾). As an example, Fig. 2 shows the shape of the $f_n(x)$ for alpha particles with $E_0 = 2$ MeV, in the case $R_0/b = .5$, $R_0/c = .1$, and in the limit case $R_0/b = R_0/c = 0$.

Expressions (11a) and (11b) can be easily integrated if the well known empirical relation $R = x^{3/2}$ is used. The following functions are obtained

6.

$$(12a) \quad \alpha_n(x) = [2/\pi] \left[(3/2) A_n(x) - x^{n+3/2} \sqrt{1-x} \right],$$

$$(12b) \quad \beta_n(x) = \frac{3}{2n+3} \sqrt{x} - \frac{2n+6}{2n+3} x^{n+2} + (3/2) t_n(x),$$

where

$$(13a) \quad A_n(x) = \int_x^1 y^n \sqrt{(1-y)(y-x)} dy = \frac{2n+1}{2n+4} (1+x) \beta_{n-1}(x) - \frac{n-1}{n-2} x \beta_{n-2}(x),$$

$$(13b) \quad \beta_0(x) = (\pi/8) (1-x)^2,$$

$$(13c) \quad t_n(x) = \int_x^1 y^n \sqrt{y(y-x)} dy = \frac{(1-x)^{3/2}}{n+2} + \frac{2n+1}{2n+4} x t_{n-1}(x),$$

$$(13d) \quad t_0(x) = (1/4) (2-x) \sqrt{1-x} - (x^2/8) \ln \frac{2-x+2\sqrt{1-x}}{x}.$$

No simple analytic form can be obtained for the $\mathcal{F}_n(x)$. In Figs. 3 and 4 $\alpha_0(x)$ and $\beta_0(x)$, calculated by formulas (12), are compared with curves obtained from Tables I ($E_0 =$ maximum energy of the recoiling alpha particles = 1 MeV) and IV ($E_0 = 8$ MeV). It can be verified that the approximation $R = x^{3/2}$ can be satisfactorily used if (i) $E = E_0 x$ is higher than about 0.4 MeV (for lower energies R is roughly proportional to $x^{3/4}$); in fact Figs. 3 and 4 show a better agreement for the higher energy, and the higher x values; (ii) in

Eq. (10) the term in $\gamma_n(x)$ is negligible in comparison with those in $\alpha_n(x)$ and $\beta_n(x)$. In practical cases these conditions are often satisfied because (i) experimental measurements cannot explore very low angles ($x = 0.1$ corresponds to $\theta \sim 36^\circ$); (ii) R_0 is small compared with the dimensions of the chamber, so that the term proportional to $R_0^2/(bc)$ can be neglected.

In conclusion, expressions (12) can be widely employed in practice, in spite of the approximation involved. The advantage of an analytic form for the $f_n(x)$ is relevant, especially when electronic computers are used for calculations.

It is interesting to note that the effect of induction of positive ions (Section 3) is important for big chambers ($b \gg a$), while the wall effects (Section 4) are obviously of interest for small chambers (b not very large in comparison with R_0). This is a fortunate circumstance because a simultaneous application of both corrections turns out to be cumbersome, owing to the double integration required.

5. The response of a chamber to a monoenergetic beam of ions is in general a spread line, whose shape can be well approximated by a gaussian distribution $\exp[-(hx)^2]$. If the constant h , which gives a measure of the total resolving power of the system of detection (chamber+electronic chain), can be experimentally determined, one can use the following expressions, obtained by introducing the Gaussian form in Eq. (6).

$$(14) \quad f_n(x) = \pi^{-1/2} \sum_{i=0}^n \frac{n!}{i!(n-i)!} x^{n-i} \left\{ \eta_i(h-hx) + (-)^{n+i} \eta_i(h+hx) + (-)^i [1-(-)^n] \eta_i(hx) \right\},$$

where

$$(15a) \quad \eta_i(u) = \frac{i-1}{2h^2} \eta_{i-2}(u) - \frac{1}{2h} \left(\frac{u}{h}\right)^{i-1} \exp[-u^2],$$

$$(15b) \quad \eta_1(u) = -\frac{1}{2h} \exp[-u^2],$$

$$(15c) \quad \mathcal{I}_0(u) = (\sqrt{\pi}/2) \phi(u)$$

$(\phi(u) = (2/\sqrt{\pi}) \int_0^u \exp[-u^2] du$ is the error integral, tabulated by Jahnke and Emde). Fig. 5 shows the behaviour of $f_n(x)$ for $h = 10$ and $h = \infty$, up to P waves. If the h value is sufficiently high, as it is in practical cases, the effect concerns only forward and backward scattering angles ($x \sim 0$ and $x \sim 1$), the remaining part of the spectrum being unaltered. At the highest scattering angles ($x \sim 1$) the effect has particular interest, because it is responsible for the tail which is observed in experimental angular distributions. The corrections to this tail can be evaluated exactly by Eq. (14), or by the following approximate expression, which can be used for h higher than about 5 and hx higher than about 2:

$$(16) \quad f_n(x) = x^n \frac{\phi(h-hx) + 1}{2} - \frac{n x^{n-1}}{2h\sqrt{\pi}} \exp[-(h-hx)^2].$$

Bibliography

- (1) - F. Demanins, G. Pisent, G. Poiani and C. Villi, Phys. Rev. 125, 318 (1962);
- (2) - R. Malaroda, G. Poiani and G. Pisent, Phys. Letters 5, 205 (1963);
- (3) - D. H. Wilkinson, (Cambridge, 1960);
- (4) - B. Rossi and H. H. Staub, (McGraw-Hill 1949);
- (5) - T. H. R. Skyrme, P. R. Tunncliffe and A. G. Ward, Rev. Sci. Instr. 23, 204 (1952);
- (6) - P. R. Tunncliffe, Phys. Rev. 89, 1247 (1953);
- (7) - H. A. Bethe, Rev. Modern Phys. 22, 213 (1950);
- (8) - W. Whaling, Handbuch der Physik, (Springer Verlag, 1958), vol. 34, p. 193.

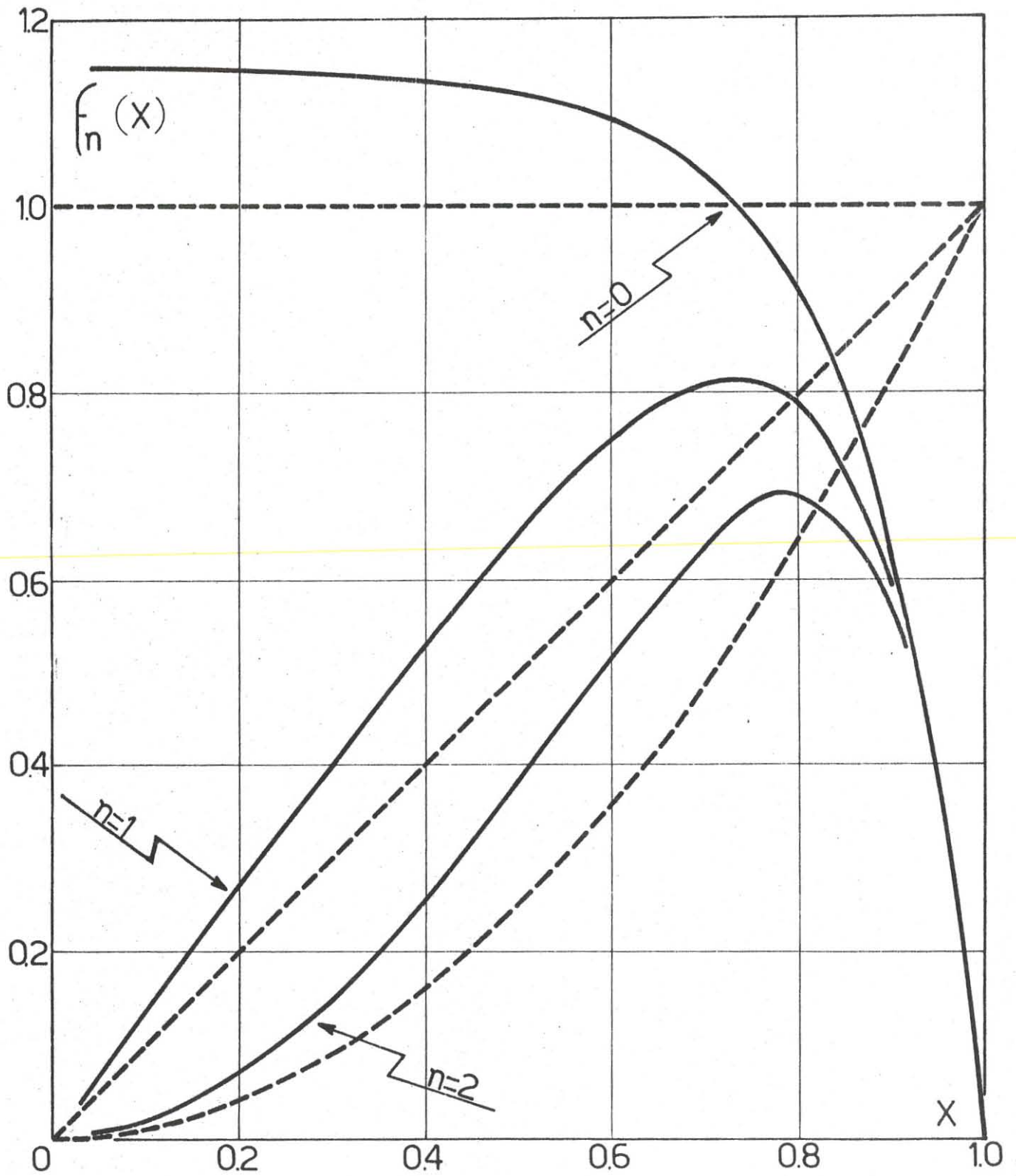


FIG. 1

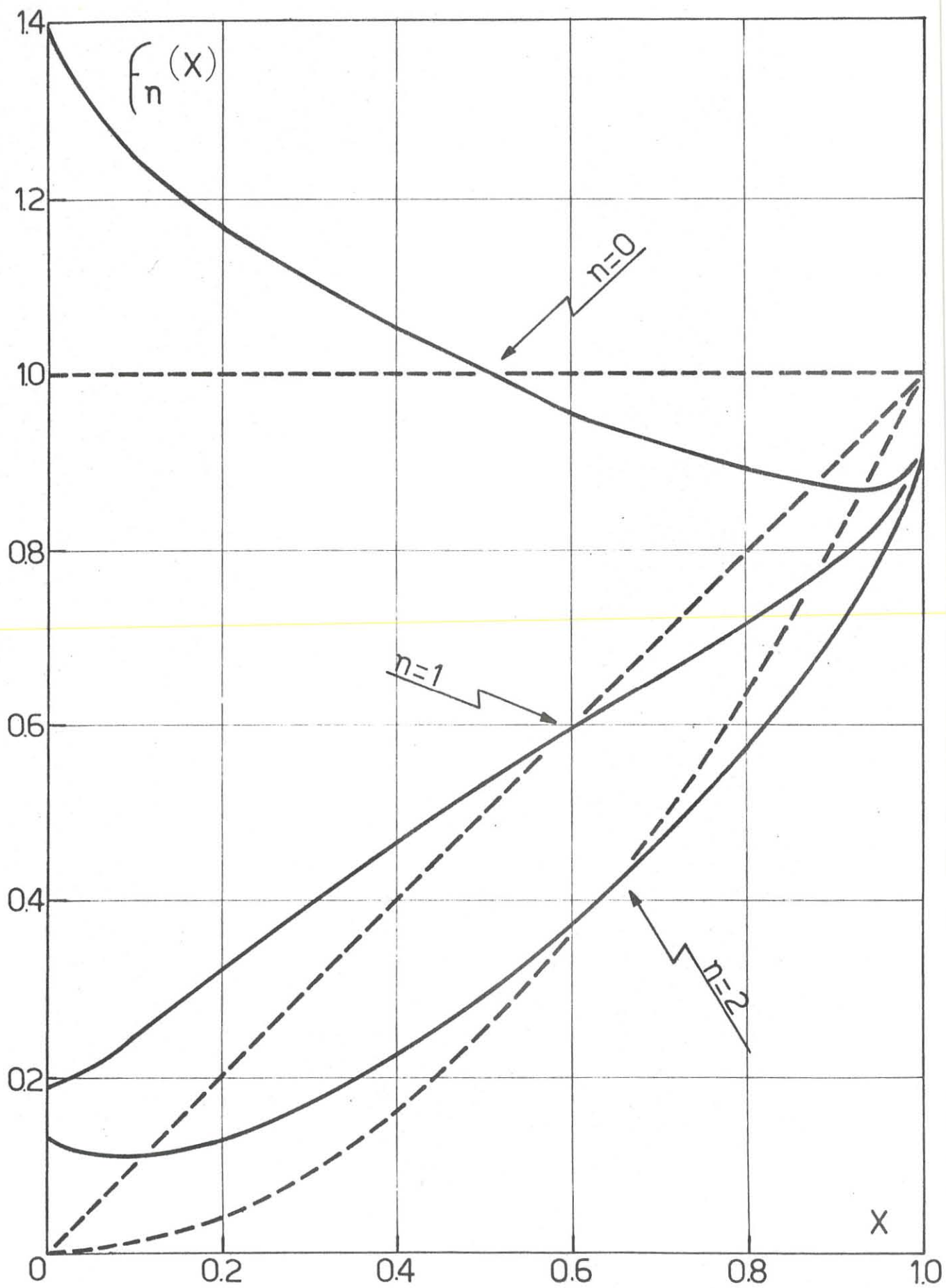


FIG. 2

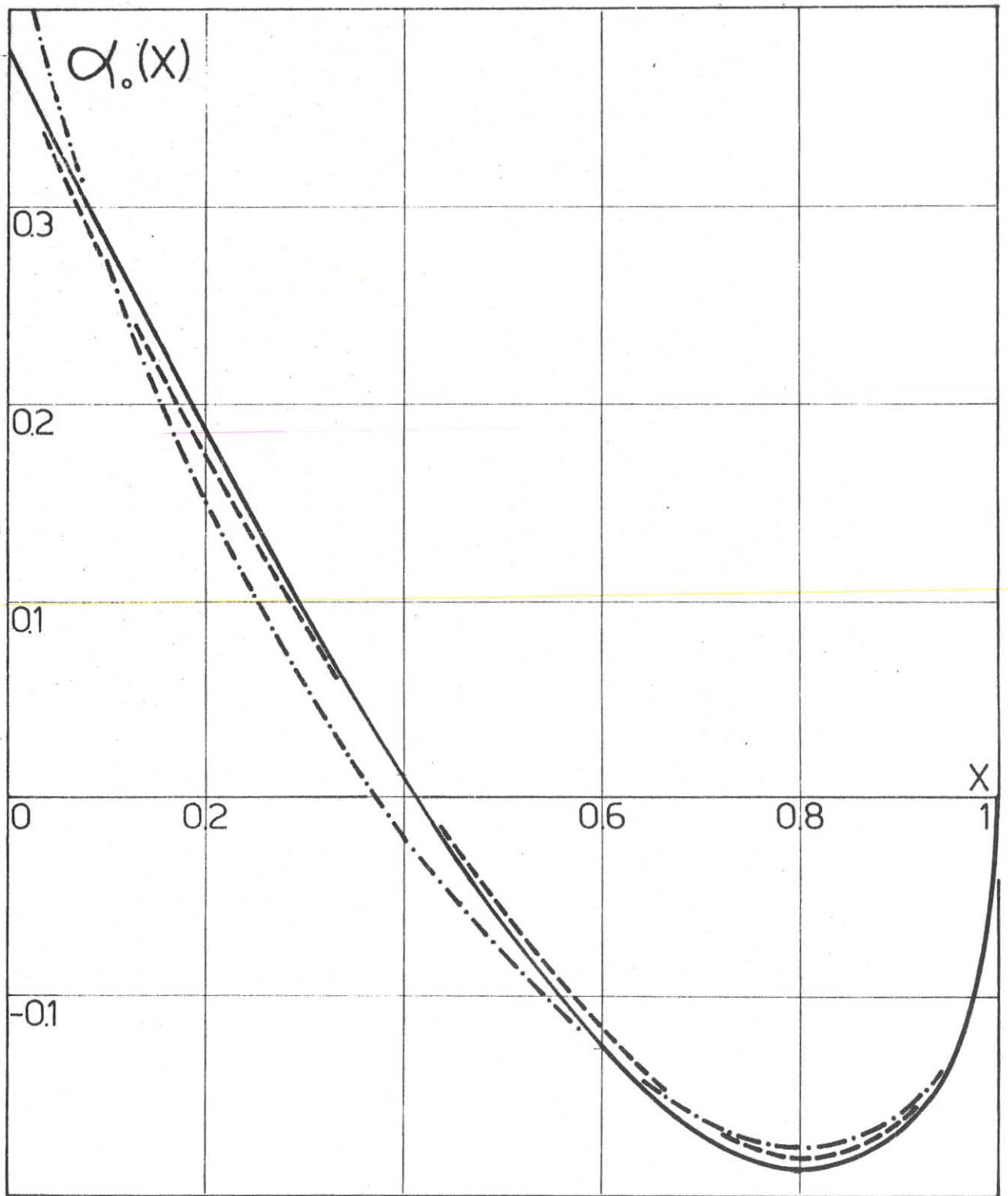


FIG. 3

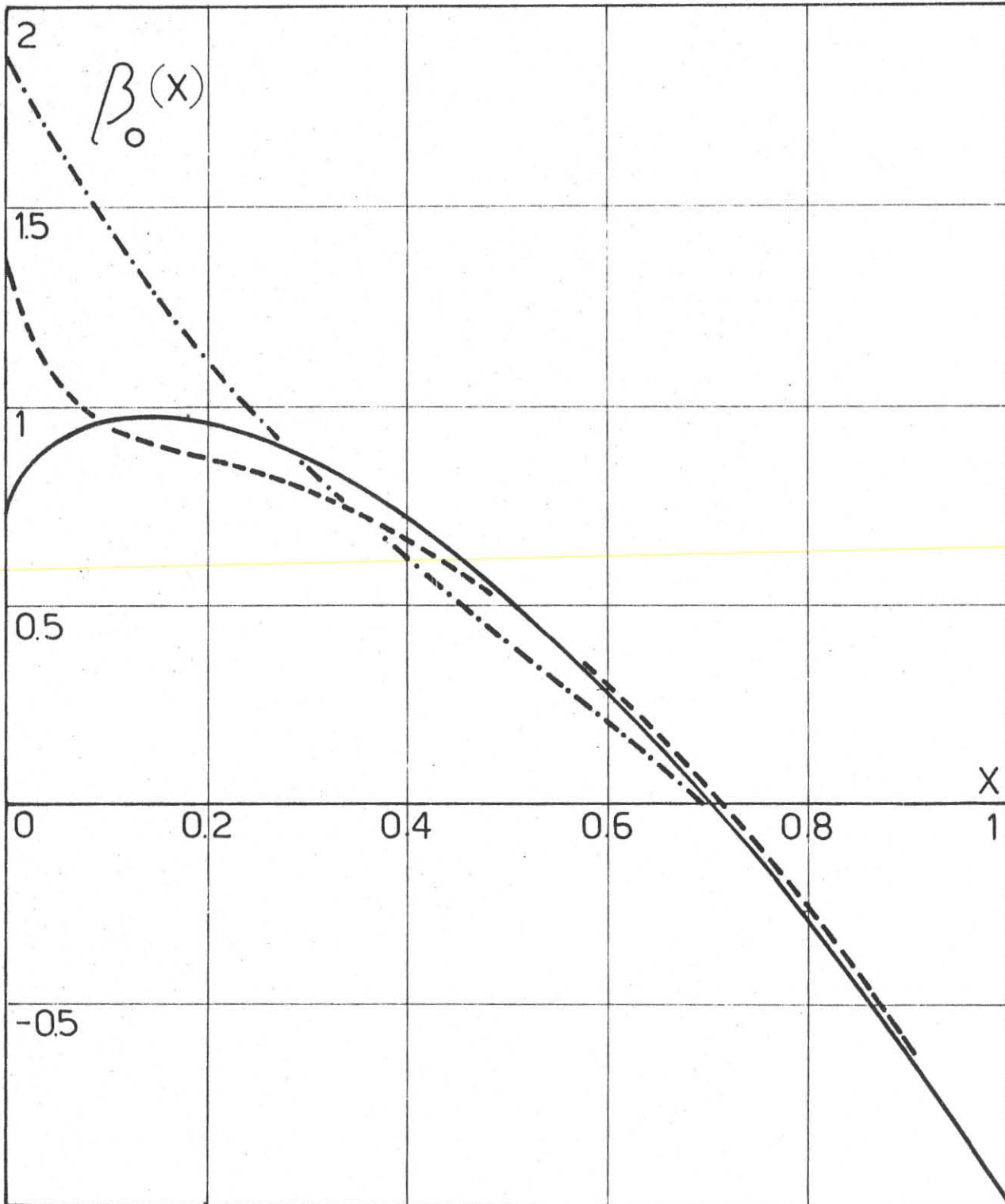
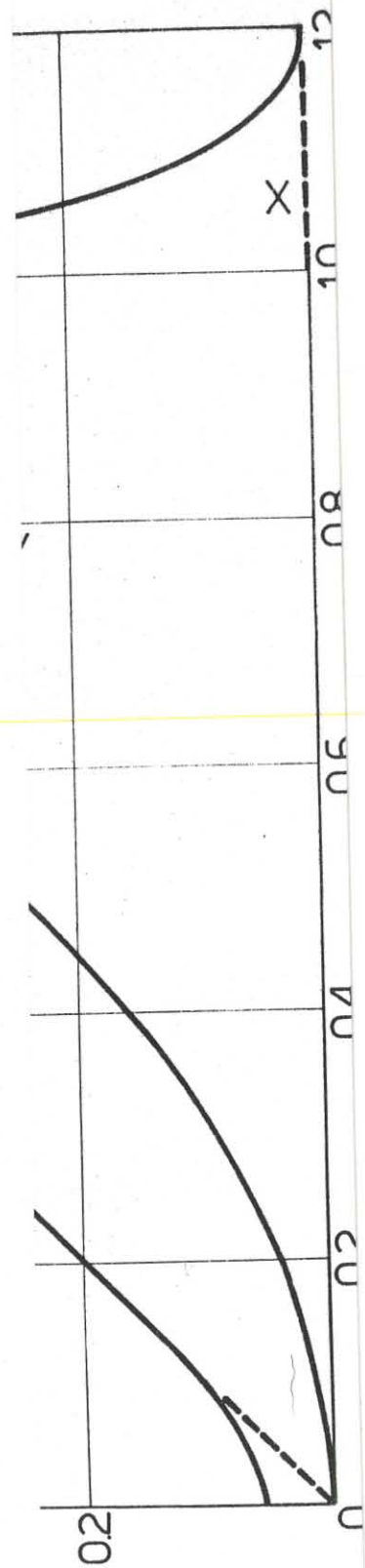


FIG. 4



5

TABLE I

 $E_0 = 1 \text{ MeV}$

	x	n=0	n=1	n=2	n=3	n=4
a_n	0	0.441	0.148	0.081	0.054	0.038
	0.1	0.275	0.142	0.082	0.054	0.039
	0.2	0.148	0.116	0.077	0.053	0.039
	0.3	0.055	0.080	0.066	0.050	0.038
	0.4	-0.021	0.036	0.046	0.042	0.035
	0.5	-0.081	-0.010	0.017	0.026	0.027
	0.6	-0.128	-0.058	-0.020	0.000	0.010
	0.7	-0.162	-0.103	-0.064	-0.037	-0.020
	0.8	-0.177	-0.137	-0.106	-0.081	-0.062
	0.9	-0.161	-0.144	-0.129	-0.115	-0.103
	1.0	0	0	0	0	0
B_n	0	1.867	1.097	0.780	0.606	0.493
	0.1	1.450	0.895	0.625	0.495	0.395
	0.2	1.096	0.741	0.540	0.421	0.344
	0.3	0.850	0.637	0.487	0.385	0.316
	0.4	0.610	0.516	0.424	0.350	0.292
	0.5	0.421	0.410	0.370	0.325	0.283
	0.6	0.212	0.265	0.277	0.269	0.252
	0.7	-0.019	0.072	0.127	0.158	0.173
	0.8	-0.285	-0.183	-0.105	-0.046	-0.001
	0.9	-0.614	-0.539	-0.473	-0.414	-0.361
	1.0	-1.000	-1.000	-1.000	-1.000	-1.000
γ_n	0	-0.103	-0.066	-0.046	-0.034	-0.027
	0.1	-0.118	-0.064	-0.040	-0.027	-0.019
	0.2	-0.124	-0.072	-0.046	-0.032	-0.024
	0.3	-0.122	-0.080	-0.054	-0.039	-0.029
	0.4	-0.101	-0.077	-0.058	-0.044	-0.033
	0.5	-0.077	-0.070	-0.059	-0.049	-0.040
	0.6	-0.038	-0.047	-0.047	-0.044	-0.040
	0.7	0.013	-0.007	-0.018	-0.024	-0.027
	0.8	0.068	0.047	0.031	0.018	0.009
	0.9	0.112	0.099	0.088	0.077	0.068
	1.0	0	0	0	0	0

TABLE II

 $E_0 = 2 \text{ MeV}$

	x	n=0	n=1	n=2	n=3	n=4
a_n	0	0.412	0.160	0.094	0.064	0.047
	0.1	0.252	0.145	0.089	0.061	0.045
	0.2	0.147	0.116	0.081	0.057	0.043
	0.3	0.060	0.070	0.066	0.051	0.040
	0.4	-0.014	0.035	0.044	0.041	0.035
	0.5	-0.078	-0.013	0.013	0.023	0.024
	0.6	-0.129	-0.062	-0.025	-0.005	0.005
	0.7	-0.163	-0.107	-0.068	-0.042	-0.025
	0.8	-0.178	-0.139	-0.109	-0.085	-0.065
	0.9	-0.160	-0.144	-0.129	-0.115	-0.103
	1.0	0	0	0	0	0
B_n	0	1.911	1.154	0.833	0.652	0.534
	0.1	1.215	0.774	0.561	0.441	0.363
	0.2	0.963	0.664	0.493	0.389	0.320
	0.3	0.803	0.605	0.467	0.374	0.310
	0.4	0.634	0.529	0.435	0.361	0.305
	0.5	0.447	0.422	0.378	0.331	0.290
	0.6	0.226	0.267	0.274	0.265	0.248
	0.7	0.002	0.082	0.130	0.156	0.169
	0.8	-0.274	-0.180	-0.107	-0.052	-0.009
	0.9	-0.582	-0.511	-0.448	-0.392	-0.342
	1.0	-1.000	-1.000	-1.000	-1.000	-1.000
γ_n	0	-0.115	-0.072	-0.050	-0.038	-0.029
	0.1	-0.075	-0.042	-0.028	-0.020	-0.015
	0.2	-0.090	-0.055	-0.037	-0.026	-0.020
	0.3	-0.104	-0.071	-0.050	-0.037	-0.028
	0.4	-0.101	-0.078	-0.060	-0.046	-0.036
	0.5	-0.079	-0.071	-0.060	-0.050	-0.041
	0.6	-0.039	-0.045	-0.046	-0.043	-0.039
	0.7	-0.010	-0.007	-0.017	-0.022	-0.025
	0.8	0.067	0.048	0.033	0.021	0.012
	0.9	0.108	0.096	0.085	0.075	0.066
	1.0	0	0	0	0	0

TABLE III

 $E_0 = 4 \text{ MeV}$

	x	n=0	n=1	n=2	n=3	n=4
α_n	0	0.390	0.176	0.110	0.076	0.058
	0.1	0.258	0.153	0.099	0.070	0.052
	0.2	0.161	0.122	0.086	0.062	0.047
	0.3	0.075	0.083	0.068	0.053	0.042
	0.4	0.000	0.038	0.044	0.040	0.034
	0.5	-0.066	-0.010	0.013	0.021	0.023
	0.6	-0.120	-0.059	-0.025	-0.006	-0.004
	0.7	-0.159	-0.106	-0.069	-0.044	-0.027
	0.8	-0.177	-0.140	-0.110	-0.086	-0.068
	0.9	-0.161	-0.145	-0.130	-0.116	-0.104
	1.0	0	0	0	0	0
β_n	0	1.623	1.015	0.744	0.588	0.486
	0.1	1.032	0.683	0.507	0.404	0.336
	0.2	0.877	0.619	0.469	0.376	0.313
	0.3	0.759	0.577	0.452	0.367	0.307
	0.4	0.632	0.524	0.431	0.360	0.305
	0.5	0.457	0.424	0.377	0.331	0.290
	0.6	0.272	0.298	0.296	0.281	0.261
	0.7	0.025	0.097	0.139	0.163	0.173
	0.8	-0.245	-0.157	-0.089	-0.037	0.002
	0.9	-0.583	-0.514	-0.452	-0.397	-0.348
	1.0	-1.000	-1.000	-1.000	-1.000	-1.000
γ_n	0	-0.054	-0.031	-0.022	-0.016	-0.012
	0.1	-0.039	-0.022	-0.014	-0.010	-0.007
	0.2	-0.073	-0.046	-0.032	-0.024	-0.018
	0.3	-0.096	-0.068	-0.049	-0.037	-0.029
	0.4	-0.103	-0.079	-0.061	-0.048	-0.039
	0.5	-0.085	-0.074	-0.062	-0.052	-0.043
	0.6	-0.053	-0.054	-0.052	-0.047	-0.042
	0.7	0.000	-0.013	-0.021	-0.025	-0.026
	0.8	0.059	0.041	0.028	0.017	-0.010
	0.9	0.107	0.095	0.084	0.065	0.046
	1.0	0	0	0	0	0

TABLE IV

 $E_0 = 8 \text{ MeV}$

	x	n=0	n=1	n=2	n=3	n=4
α_n	0	0.378	0.189	0.120	0.085	0.064
	0.1	0.268	0.162	0.106	0.076	0.058
	0.2	0.177	0.128	0.091	0.067	0.052
	0.3	0.092	0.089	0.072	0.057	0.045
	0.4	0.012	0.042	0.046	0.042	0.036
	0.5	-0.059	-0.008	0.013	0.021	0.022
	0.6	-0.118	-0.060	-0.027	-0.009	0.002
	0.7	-0.161	-0.108	-0.072	-0.047	-0.030
	0.8	-0.180	-0.143	-0.113	-0.089	-0.070
	0.9	-0.163	-0.147	-0.132	-0.118	-0.106
	1.0	0	0	0	0	0
β_n	0	1.365	0.879	0.652	0.520	0.435
	0.1	0.949	0.646	0.487	0.391	0.326
	0.2	0.869	0.623	0.477	0.385	0.322
	0.3	0.793	0.604	0.477	0.389	0.328
	0.4	0.655	0.540	0.446	0.374	0.319
	0.5	0.505	0.458	0.403	0.353	0.309
	0.6	0.304	0.321	0.314	0.296	0.274
	0.7	0.045	0.112	0.151	0.172	0.181
	0.8	-0.255	-0.167	-0.099	-0.047	-0.007
	0.9	-0.620	-0.549	-0.486	-0.429	-0.378
	1.0	-1.000	-1.000	-1.000	-1.000	-1.000
γ_n	0	-0.002	-0.002	-0.003	-0.003	-0.003
	0.1	-0.022	-0.011	-0.006	-0.004	-0.002
	0.2	-0.071	-0.047	-0.033	-0.025	-0.019
	0.3	-0.104	-0.074	-0.055	-0.043	-0.034
	0.4	-0.110	-0.085	-0.066	-0.053	-0.043
	0.5	-0.098	-0.083	-0.069	-0.058	-0.048
	0.6	-0.063	-0.061	-0.057	-0.051	-0.045
	0.7	-0.006	-0.017	-0.024	-0.027	-0.028
	0.8	0.059	0.042	0.029	0.019	0.011
	0.9	0.108	0.086	0.075	0.066	0.047
	1.0	0	0	0	0	0